J|A|C|S ARTICLES

Published on Web 12/12/2008

Reversible Phototuning of the Large Anisotropic Magnetization at the Interface between a Self-Assembled Photochromic Monolayer and Gold

Masayuki Suda, Naoto Kameyama, Aya Ikegami, and Yasuaki Einaga*

Department of Chemistry, Faculty of Science and Technology, Keio University, 3-14-1 Hiyoshi, Yokohama 223-8522, Japan

Received October 20, 2008; E-mail: einaga@chem.keio.ac.jp

Abstract: We have observed the emergence of a large anisotropic magnetization and significant photoinduced changes in the magentization that appear at the interface between a gold film and an azobenzene-containing self-assembled monolayer. The magnetization value was extremely high, up to 50 μ_B per adsorbed molecule. These photomagnetic effects can be attributed to a photoinduced change in the loss of d charge due to photoisomerization of the azobenzene monolayer, which is accompanied by inversion of the surface dipoles. Furthermore, we have also observed reversible changes in the work function of the gold film by alternating UV and visible light, showing that the value of the surface dipole moment is changed as a result of photoisomerization. This allowed us to control the magnetization by alternating the photoillumination between UV and visible light, and we have clarified the mechanism for these photomagnetic effects. A novel strategy such as this, which enables significant reversible phototuning of the magnetic order, has great potential for applications in future magneto-optical devices.

Introduction

The formation of an organic self-assembled monolayer (SAM) on a metal surface gives rise to novel functionalities as a result of the ability of the monolayer to modify the electronic properties of the metal surface.[1−5] These effects arise because of charge transfer at the organic−inorganic interface required to equalize the electrochemical potentials of the adsorbate and substrate. Specifically, thiolated adsorbates adsorbed on gold surfaces have been studied extensively, and electron transfer from the gold to the thiols has been shown both theoretically and experimentally.[6−10] A recent good example of the novel properties resulting from the formation of a SAM on gold is the emergence of paramagnetism or ferromagnetism in thiol-passivated gold films and gold nanoparticles despite their bulk diamagnetic component. Since its discovery by Naaman and co-workers, the occurrence of magnetism at Au−S interfaces has been reported in a number of recent papers.[11−13] Furthermore, Crespo et al.[12a] have demonstrated ferromagnetism in thiol-passivated gold nanoparticles even at room temperature. The magnetism is associated with Au 5d localized holes that are the result of charge transfer from the Au surface atoms to the S atoms of the organic ligands during formation of the Au−S bonds.

Another important advantage that can be gained by using this kind of magnetic compound is the strong possibility of incorporating secondary functionality, such as phototunability, into the magnetic system through the use of functional molecules

(1) (a) Ishii, H.; Sugiyama, K.; Ito, E.; Seki, K. *Adv. Mater.* **1999**, *11*, 605. (b) Yaliraki, S. N.; Roitberg, A. E.; Gonzalez, C.; Mujica, V.; Ratner, M. A. *J. Chem. Phys.* **1999**, *111*, 6997.

(2) (a) Vilan, A.; Shanzer, A.; Cahen, D. *Nature* **2000**, *404*, 166. (b) Campbell, I. H.; Kress, J. D.; Martin, R. L.; Smith, D. L.; Barashkov, N. N.; Ferraris, J. P. *Appl. Phys. Lett.* **1997**, *71*, 3528. (c) Hill, I. G.; Milliron, D.; Schwartz, J.; Kahn, A. *Appl. Surf. Sci.* **2000**, *166*, 354.

(3) (a) Collier, C. P.; Wong, E. W.; Belohradsky, M.; Raymo, F. M.; Stoddart, J. F.; Kuekes, P. J.; Williams, R. S.; Heath, J. R. *Science* **1999**, *285*, 391. (b) Chen, J.; Reed, M. A.; Rawlett, A. M.; Tour, J. M. *Science* **1999**, *286*, 1550. (c) Vuillaume, D.; Chen, B.; Metzger, R. M. *Langmuir* **1999**, *15*, 4011. (d) Punkka, E.; Rubner, R. F. *J. Electron. Mater.* **1992**, *21*, 1057.

(4) (a) Yamamori, A.; Hayashi, S.; Koyama, T.; Taniguchi, Y. *Appl. Phys. Lett.* **2001**, *78*, 3343. (b) Crone, B. K.; Davids, P. S.; Campbell, I. H.; Smith, D. L. *J. Appl. Phys.* **2000**, *87*, 1974. (c) Boer, B.; Hadipour, A.; Mandoc, M. M.; Woudenbergh, T.; Brom, P. W. M. *Adv. Mater.* **2005**, *17*, 621.

(5) Wu, D. G.; Cahen, D.; Graf, P.; Naaman, R.; Nitzan, A.; Shvarts, D. *Chem.−Eur. J.* **2001**, *7*, 1743.

(6) Ray, S. G.; Cohen, H.; Naaman, R.; Liu, H.; Waldeck, D. H. *J. Phys. Chem. B* **2005**, *109*, 14064.

(7) Alloway, D. M.; Hofmann, M.; Smith, D. L.; Gruhn, N. E.; Graham, A. L.; Colorado, R., Jr.; Wysocki, V. H.; Lee, T. R.; Lee, P. A.; Armstrong, N. R. *J. Phys. Chem. B* **2003**, *107*, 11690.

(8) Andreoni, W.; Curioni, A.; Grönbeck, H. *Int. J. Quantum Chem.* **2000**, *80*, 598.

(9) Sellers, H.; Ulman, A.; Shnidman, Y.; Eilers, J. E. *J. Am. Chem. Soc.* **1993**, *115*, 9389.

(10) Caruso, A. N.; Wang, L. G.; Jaswal, E. Y.; Tsymbal, E. Y.; Dowben, P. A. *J. Mater. Sci.* **2006**, *41*, 6198.

(11) (a) Carmeli, I.; Leitus, G.; Naaman, R.; Reich, S.; Vager, Z. *J. Chem. Phys.* **2003**, *118*, 10372. (b) Hernando, A.; Crespo, P.; García, M. A.; Pinel, E. F.; Venta, J.; Fernández, A.; Penadés, S. *Phys. Rev. B* **2006**, *74*, 052403.

(12) (a) Crespo, P.; Litrán, R.; Rojas, T. C.; Multigner, M.; Fuente, J. M.; Sánchez-López, J. C.; García, M. A.; Hernando, A.; Penadés, S.; Fernández, A. *Phys. Rev. Lett.* **2004**, *93*, 087204. (b) Negishi, Y.; Tsunoyama, H.; Suzuki, M.; Kawamura, N.; Matsushita, M. M.; Maruyama, K.; Sugawara, T.; Yokoyama, T.; Tsukuda, T. *J. Am. Chem. Soc.* **2006**, *128*, 12034. (c) Dutta, P.; Pal, S.; Seehra, M. S.; Anand, M.; Roberts, C. B. *Appl. Phys. Lett.* **2007**, *90*, 213102. (d) Garitaonandia, J. S.; Insausti, M.; Goikolea, E.; Suzuki, M.; Cashion, J. D.; Kawamura, N.; Ohsawa, H.; Muro, I. G.; Suzuki, K.; Plazaola, F.; Rojo, T. *Nano Lett.* **2008**, *8*, 661.

(13) Suda, M.; Kameyama, N.; Suzuki, M.; Kawamura, N.; Einaga, Y. *Angew. Chem., Int. Ed.* **2008**, *47*, 160.

as organic components, since the charge transfer from Au to S atoms acts as a trigger for the generation of magnetism, the magnitude of which is dependent on the electronic structure of the adsorbates.[13] Recently, the design of molecular compounds that exhibit photoinduced magnetization and magnetic transitions is one of the main challenges in the field of material science because of their potential for applications in future optical memory and switching devices.[14−21]

In our previous paper,[13] we reported the design of gold nanoparticles passivated with azobenzene-derivatized thiols. Since the charge transfer from Au to S atoms acts as a "trigger" for the generation of paramagnetism, the magnitude of the magnetic moment varies with the work function of the metal. It is well-known that the metal work function is correlated with the surface dipole moment of the organic layer, which arises from the cooperative effect of the intrinsic molecular dipoles. Since the trans and cis states of azobenzene-derivatized thiols have opposite dipoles, they can be used to decrease and increase, respectively, the work function of gold. In fact, this system demonstrated reversible photocontrol of the ferromagnetism even at room temperature. However, the mechanisms for explaining such photomagnetic phenomena are less well elucidated.[13]

In this work, we have designed an azobenzene-containing SAM on a gold film. At the interface between the gold and the SAM, we observed the emergence of a large anisotropic magnetization as well as significant photoinduced changes in the magnetization value when alternating between UV and visible light illumination. Furthermore, we also observed reversible changes in a new absorption band near 800 nm arising from electron transfer as well as reversible changes in the work function of the gold film by illumination, showing that the value of the surface dipole layer changes as a result of photoisomerization. These photomagnetic effects can be attributed to photoinduced changes in the amount of charge transfer by photoisomerization of the azobenzene monolayer, which is accompanied by inversion of the surface dipoles.

As a result, we succeeded in controlling the magnetization by alternating the photoillumination between UV and visible light, and we have clarified the mechanism for the photomagnetic effects.

Experimental Section

Synthesis of the Asymmetrical Azobenzene Disulfide. The photoreactive SAM consisted of the asymmetrical azobenzene disulfide 4-[6-(hexyldithio)hexyloxy]azobenzene (AZ), which had been designed and synthesized to realize a surface photoisomerization reaction. AZ was synthesized in a similar manner to that in a previous report.[22]

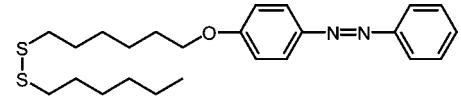

AZ

SAM Preparation. The substrates were glass coverslips coated with a 10 nm thick layer of gold, which had been purchased from Aldrich. The gold surface shows a tendency toward the (111) orientation that can be greatly enhanced by annealing at 400 °C for 8 h (see Figure S1 in the Supporting Information). Prior to SAM deposition, the prepared gold substrates were cleaned by immersion in a "piranha" solution consisting of 70% H_2SO_4 and 30% H_2O_2. After the substrates were cleaned, they were immediately and thoroughly rinsed in high-resistivity water and in ethanol that had been treated to remove organic impurities. To deposit monolayers, the cleaned substrates were submerged in a 1 mM solution of AZ in dichloromethane for 24 h at room temperature. After deposition, the substrates were thoroughly rinsed with dichloromethane and ethanol and then dried in gently-flowing argon. We refer to these SAM-deposited gold substrates as AZ-SAM.

Physical Methods. UV/vis spectra were recorded on a V-560 spectrometer (JASCO). The UV illumination (filtered light, $\lambda_{max} =$ 360 nm, 1.0 mW cm^{-2}) was obtained from an ultrahigh pressure mercury lamp (HYPERCURE 200, Yamashita Denso). Visible light (400−700 nm, 1.0 mW cm^{-2}) was provided by a xenon lamp (XFL-300, Yamashita Denso). Reflection−absorption infrared spectroscopy (IRAS) was performed in the reflection mode (angle of incidence: 80° to the surface normal) using a p-polarized beam on a FT/IR 660 plus instrument (JASCO) equipped with a polarizer. The magnetic properties were investigated with a SQUID magnetometer (model MPMS-XL, Quantum Design). Light was guided into the SQUID magnetometer by an optical fiber to study the photomagnetic effects. X-ray diffraction patterns were recorded on a D8 ADVANCE diffractometer (Bruker) using Ni-filtered Cu Kα radiation. Measurements of the work function were performed in KFM mode with a SPM-9600 instrument (Shimadzu).

Results and Discussion

Characterization of the AZ-SAM. Figure 1 shows the IR spectrum of the bulk AZ powder in a KBr pellet recorded in transmission mode and that of the AZ-SAM recorded in IRAS mode. Absorption peaks attributed to $\nu_{as}(CH_3)$, $\nu_{as}(CH_2)$, $\nu_s(CH_3)$, and $\nu_s(CH_2)$ are observed at 2957, 2919, 2874, and 2850 cm^{-1} in the spectrum of the bulk AZ (Figure 1a), while only the peaks attributed to $\nu_{as}(CH_2)$, $\nu_s(CH_3)$, and $\nu_s(CH_2)$ are observed at 2919, 2874, and 2850 cm^{-1} in the spectrum of the AZ-SAM (Figure 1b).[23] It is well-known that the frequencies of the methylene stretching bands are sensitive to the conforma-

(14) (a) Sato, O.; Iyoda, T.; Fujishima, A.; Hashimoto, K. *Science* **1996**, *272*, 704. (b) Sato, O.; Einaga, Y.; Iyoda, T.; Fujishima, A.; Hashimoto, K. *J. Electrochem. Soc.* **1997**, *144*, L11. (c) Ohkoshi, S.; Yorozu, S.; Sato, O.; Iyoda, T.; Fujishima, A.; Hashimoto, K. *Appl. Phys. Lett.* **1997**, *70*, 1040. (d) Yamamoto, Y.; Umemura, Y.; Sato, O.; Einaga, Y. *J. Am. Chem. Soc.* **2005**, *127*, 16065. (e) Taguchi, M.; Yagi, I.; Nakagawa, M.; Iyoda, T.; Einaga, Y. *J. Am. Chem. Soc.* **2006**, *128*, 10978.
(15) (a) Decurtins, S.; Gütlich, P.; Kohler, C. P.; Spiering, H.; Hauser, A. *Chem. Phys. Lett.* **1984**, *105*, 1. (b) Renz, F.; Oshio, H.; Ksenofontov, V.; Waldeck, M.; Spiering, H.; Gütlich, P. *Angew. Chem., Int. Ed.* **2000**, *39*, 3699. (c) Hayami, S.; Gu, Z.-Z.; Shiro, M.; Einaga, Y.; Fujishima, A.; Hashimoto, K. *J. Am. Chem. Soc.* **2000**, *122*, 7126.
(16) Gütlich, P.; Garcia, Y.; Woike, T. *Coord. Chem. Rev.* **2001**, *219*, 839.
(17) Matsuda, K.; Irie, M. *J. Am. Chem. Soc.* **2000**, *122*, 7195.
(18) (a) Koshihara, S.; Oiwa, A.; Hirasawa, M.; Katsumoto, S.; Iye, Y.; Urano, C.; Takagi, H.; Munekata, H. *Phys. Rev. Lett.* **1997**, *78*, 4617. (b) Haneda, S.; Munekata, H.; Takatani, Y.; Koshihara, S. *J. Appl. Phys.* **2000**, *87*, 6445.
(19) Matsuda, K.; Machida, A.; Moritomo, Y.; Nakamura, A. *Phys. Rev. B* **1998**, *58*, R4203.
(20) (a) Einaga, Y.; Sato, O.; Iyoda, T.; Fujishima, A.; Hashimoto, K. *J. Am. Chem. Soc.* **1999**, *121*, 3745. (b) Yamamoto, T.; Umemura, Y.; Sato, O.; Einaga, Y. *Chem. Mater.* **2004**, *16*, 1195. (c) Taguchi, M.; Yamada, K.; Suzuki, S.; Sato, O.; Einaga, Y. *Chem. Mater.* **2005**, *17*, 4554.
(21) (a) Mikami, R.; Taguchi, M.; Yamada, K.; Suzuki, K.; Sato, O.; Einaga, Y. *Angew. Chem., Int. Ed.* **2004**, *43*, 6135. (b) Suda, M.; Miyazaki, Y.; Hagiwara, Y.; Sato, O.; Shiratori, S.; Einaga, Y. *Chem. Lett.* **2005**, *34*, 1028. (c) Suda, M.; Nakagawa, M.; Iyoda, T.; Einaga, Y. *J. Am. Chem. Soc.* **2007**, *129*, 5538.
(22) (a) Akiyama, H.; Tamada, K.; Nagasawa, J.; Nakanishi, F.; Tamaki, T. *Trans. Mater. Res. Soc. Jpn.* **2000**, *25*, 425. (b) Tamada, K.; Akiyama, H.; Wei, T. X. *Langmuir* **2002**, *18*, 5239. (c) Tamada, K.; Akiyama, H.; Wei, T. X.; Kim, S. A. *Langmuir* **2003**, *19*, 2306. (d) Akiyama, H.; Tamada, K.; Nagasawa, J.; Abe, K.; Tamaki, T. *J. Phys. Chem. B* **2003**, *107*, 130.
(23) Ihs, A.; Uvdal, K.; Liedberg, B. *Langmuir* **1993**, *9*, 739.

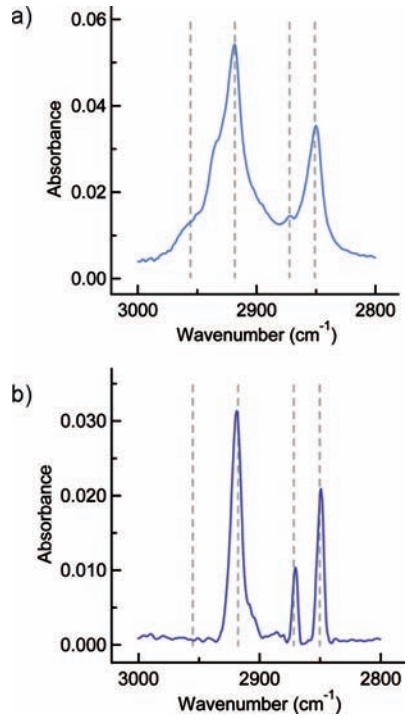

Figure 1. IR spectra of AZ in the C−H stretching mode region: (a) transmission spectrum of bulk AZ powder in a KBr pellet; (b) IRAS spectrum of the AZ-SAM on a Au film.

tion of the alkyl chain; the negligible shift in the peaks at 2919 and 2850 cm^{-1} in going from the bulk AZ spectrum to the AZ-SAM spectrum suggests that the alkyl chains in the AZ-SAM have crystalline-like packing with trans−zigzag conformation of the methylenes.[24] Furthermore, the difference between the spectra indicates the alignment of the molecules in the AZ-SAM. The presence or absence of the $\nu_{as}(CH_3)$ vibration in the AZ-SAM spectrum is interpreted as being "odd" or "even" with respect to the carbon number of the "non-azo" alkyl chains.[25,26] For the "even" case, the transition dipoles of $\nu_s(CH_3)$ and $\nu_{as}(CH_3)$ are expected to be normal and parallel to the substrate surface, respectively, assuming that the molecular tilt angle is ~30° in the AZ-SAM.

Figure 2 shows the UV−vis absorption spectra of the bare substrate (blue line) and the AZ-SAM (orange line). The spectrum of the bare substrate shows a broad absorption band centered at ~650 nm, which is attributed to the so-called surface plasmon resonance due to the itinerant character of the 5d electrons in the Au film. This band was strongly suppressed in the case of the AZ-SAM. These features are an indication of the increase in the damping of electrons due to charge localization at the film surface promoted by the strong interaction between the surface Au atoms and the thiolated AZ molecules. Similar observations were reported previously for thiol-passivated gold nanoparticles.[12a,13] In the system presented here, the reduced volume of the gold film, which is on the nanometer scale (~10 nm thickness), exposed the local surface area, i.e., the Au−S interface, as an explicit entity, similar to the reported thiol-passivated gold nanoparticles. The above observation is also consistent with the characteristic magnetic properties observed in the SQUID measurements, which are discussed later.

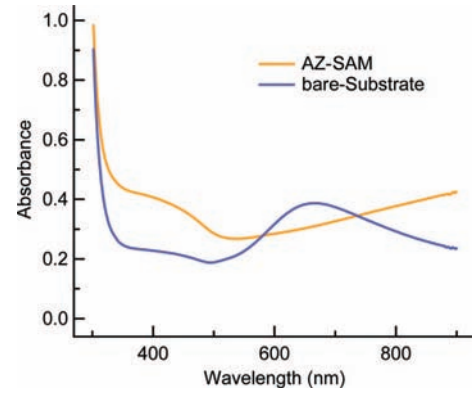

Figure 2. UV−vis absorption spectra of the bare gold substrate (blue line) and the AZ-SAM (orange line).

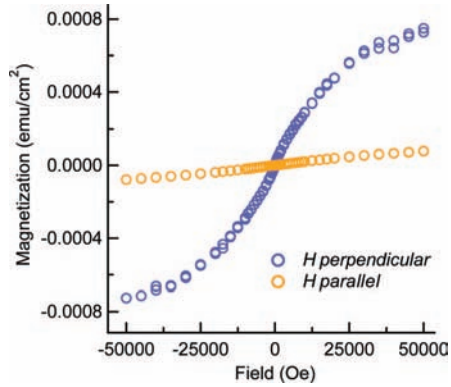

Figure 3. Plots of the magnetization M vs applied magnetic field H at 5 K for the AZ-SAM when the external magnetic field was applied perpendicular (blue points) and parallel (orange points) to the substrate surface.

Another important feature of the UV−vis absorption spectra is the emergence of a new absorption band at ~800 nm in the spectrum of the AZ-SAM, which was not observed in the spectrum of the bare substrate. Recent experimental and theoretical studies reveal that this new absorption band can be attributed to a new state arising from electron transfer at the interface between the self-assembled organized organic layer and the gold substrate that was not found in either the solid substrate itself or the organic molecules.[27,28] The emergence of this new band also reveals the formation of an organized monolayer in the AZ-SAM.

Magnetic Properties of the AZ-SAM. Figure 3 shows $M-H$ plots of the AZ-SAM after subtraction of the magnetic contribution from the bare substrate, as measured at 5 K by SQUID magnetometry. The external magnetic field was applied perpendicular (blue curve) and parallel (orange curve) to the film surface. There is a large difference between the in-plane (parallel to the film surface) and out-of-plane (perpendicular to the film surface) magnetization curves. The magnetization curve of the

(24) Wu, Y.; Zhao, B.; Xu, W.; Li, B.; Jung, Y. M.; Ozaki, Y. *Langmuir* **1999**, *15*, 4625.
(25) (a) Ulman, A. In *An Introduction to Ultrathin Organic Films*; Ulman, A., Ed.; Academic Press: Boston, 1991. (b) Ulman, A. *Chem. Rev.* **1996**, *96*, 1533.
(26) (a) Nuzzo, R. G.; Dubois, L. H.; Allara, D. L. *J. Am. Chem. Soc.* **1990**, *112*, 558. (b) Laibinis, P. E.; Whitesides, G. M.; Allara, D. L.; Tao, Y.-T.; Parikh, A. N.; Nuzzo, R. G. *J. Am. Chem. Soc.* **1991**, *113*, 7152. (c) Dubois, L. H.; Zegarski, B. R.; Nuzzo, R. G. *J. Electron Spectrosc. Relat. Phenom.* **1990**, *54−55*, 1143.
(27) Neuman, O.; Naaman, R. *J. Phys. Chem. B* **2006**, *110*, 5163.
(28) Shi, J.; Hong, B.; Prikh, A. N.; Collins, R. W.; Allara, D. L. *Chem. Phys. Lett.* **1995**, *246*, 90.

AZ-SAM in the out-of-plane direction exhibits giant paramagnetism (50 μ_B per surface gold atom), whereas that in the in-plane direction exhibits only a very small magnetization.

Recent theoretical studies have presented models to explain this enormous magnetic moment and the magnetic anisotropy: Vager and Naaman[29] have explained these phenomena in terms of the special properties of electrons transferred from the gold substrate to the organic layer as a result of adsorption. Triplet pairing of the electrons is enforced and confined within domains in the SAM layer. The quantum statistics of the triplet bosons provides a model that explains the enormous magnetic moment and anisotropy. Hernando et al.[11b] explained these observations as due to an orbital motion driven by localized charge and/or spin through spin−orbit coupling as a result of the charge transfer. The induced orbital moment gives rise to an effective field that is responsible for the giant magnetic anistropy.

Although the mechanisms are not yet completely understood and we must take many factors into consideration to explain them, it must be true that the charge transfer is a trigger for generating the paramagnetism. The spectroscopic and magnetic studies in this work are also consistent with the explanation above, which indicates the possibility for photocontrol of the magnetic properties.

Photoisomerization. The photoisomerization of the AZ-SAM at room temperature was monitored by UV−vis absorption spectroscopy. The absorption spectra were easily obtained in transmission mode because of the ultrathin thickness (~10 nm) of the AZ-SAM.[30] With the proof light normal to the substrate, only the component of the transition moment parallel to the substrate should appear in the spectra. The absence of the characteristic $\pi-\pi^*$ absorption band of *trans*-AZ at ~350 nm in Figure 2 (recorded at 0° from the angle of incidence) indicates that almost all of the azobenzene moieties are oriented in the direction normal to the substrate, because the transition moment of the characteristic $\pi-\pi^*$ absorption band of the *trans*-azobenzene moiety is almost parallel to the molecular axis.[31] Figure 4a shows the absorption spectrum of the AZ-SAM recorded at 40° from the angle of incidence in order to obtain the characteristic $\pi-\pi^*$ absorption band of *trans*-AZ. The spectrum of the initial state gives a weak absorption peak at 360 nm, which is ascribed to the $\pi-\pi^*$ transition in the trans isomer of AZ. After UV illumination of the trans isomer for 1 min, the peak decreased. Following subsequent illumination with visible light, it increased again. After the second cycle, the cis−trans photoisomerization was repeated without any attenuation of the area between the curves. These reversible spectral changes indicate reversible photoisomerization of AZ, even after formation of the SAM. Normally, photoisomerization of azobenzene-containing compounds does not occur in the solid state because of the large volume changes that are involved.[32] In fact, photoisomerization also does not occur in the absence of spacers when azobenzene-containing ligands are self-assembled on two-dimensional gold films.[33] In the system presented here, reversible photoisomerization was observed in the AZ-SAM with

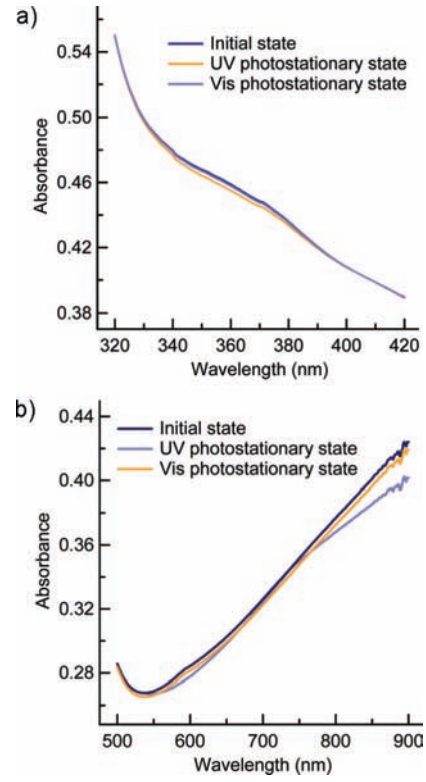

Figure 4. Changes in the UV−vis absorption spectrum for the AZ-SAM in (a) the 320−420 nm region and (b) the 500−900 nm region due to photoisomerization. The initial trans state (black line) was illuminated first with UV light for 1 min (blue line) and then with visible light for 1 min (orange line).

higher efficiency than in the case of the absence of spacers because the use of unsymmetrical azobenzene AZ provides free space between each of the azobenzene ligands, as reported previously.[22] The average distance between two neighboring nitrogen double bonds on the azobenzene ligands is estimated to be 5.0 Å for normal azobenzene-containing SAMs, while it is ~8−9 Å for the AZ-SAM (a schematic illustration is available in Figure S2 in the Supporting Information).

Furthermore, another reversible photoinduced change in the spectrum of the AZ-SAM was observed in the new absorption band at ~800 nm (Figure 4b), which is attributed to the new state arising from electron transfer at the Au−S interface that was mentioned above. Since the origin of this new band involves electron transfer, the changes in absorbance of this band seem to originate from changes in the value of the charge transfer due to photoisomerization as well as the quality of the organization of the monolayer. Though the origin of this reversible spectral change is not clear at present, it is further evidence for the reversible photoisomerization of the AZ-SAM.

Photomagnetic Effects. Subsequently, we investigated the influence of photoillumination on the magnetic properties of the AZ-SAM at 5 K (Figure 5) with an external magnetic field applied perpendicular to the film surface. During UV illumination, the initial magnetization value of the AZ-SAM decreased. Even after the illumination was stopped, the decreased magnetization value was maintained for at least several hours. We then illuminated the AZ-SAM with visible light, and the magnetization value recovered to near the value for the initial

(29) Vager, Z.; Naaman, R. *Phys. Rev. Lett.* **2004**, *92*, 087205.
(30) Sortino, S.; Petralia, S.; Conoci, S.; Belloa, S. D. *J. Mater. Chem.* **2004**, *14*, 811.
(31) (a) *Light Absorption of Organic Colorants*; Fabian, J., Hartmann, H., Eds.; Springer-Verlag: Berlin, 1980; Chapter 7. (b) Robin, M. B.; Shimpson, W. T. *J. Chem. Phys.* **1962**, *36*, 580. (c) Uznanski, P.; Kryszewsky, M.; Thuulstrup, E. W. *Spectrochim. Acta, Part A* **1990**, *46*, 23.
(32) Nakahara, H.; Fukuda, K.; Shimomura, M.; Kunitake, T. *Nippon Kagaku Kaishi* **1998**, *7*, 1001.
(33) Evans, S. D.; Johnson, S. R.; Ringsdorf, H.; Williams, L. M.; Wolf, H. *Langmuir* **1998**, *14*, 6436.

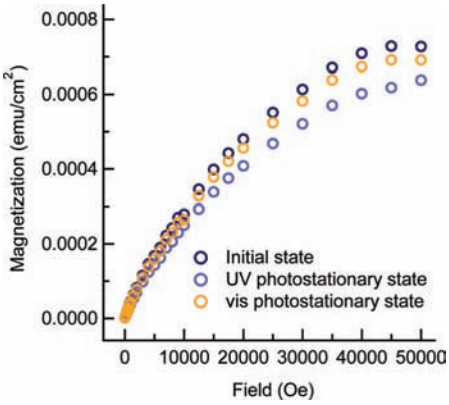

Figure 5. Plot of the magnetization M vs applied magnetic field H at 5 K for the AZ-SAM with an external magnetic field applied perpendicular to the substrate. The initial trans state (black points) was illuminated first with UV light for 1 min (blue points) and then with visible light for 1 min (orange points).

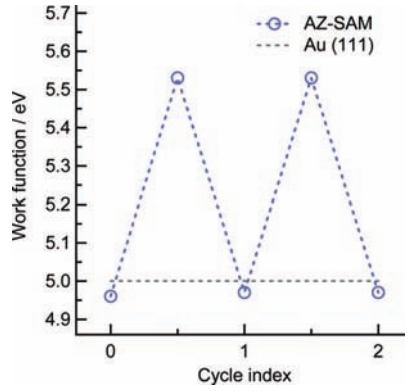

Figure 6. Change in work function of the AZ-SAM due to photoisomerization by alternating photoillumination with UV and visible light.

state. After this process, the UV-light-induced decrease and the visible-light-induced increase in magnetization were repeated without any attenuation. The photoinduced changes in the magnetization values were estimated to be ~14%.

Origin of the Photomagnetic Effects. As mentioned above, the apparent paramagnetism in the Au−S interface is associated with localized holes in the 5d shell generated by Au-to-S charge transfer through Au−S bonding. The origin of the magnetic ordering is not the large exchange interaction but rather the extremely high local magnetic anisotropy, which blocks the moments from switching.[11−13] Hence, the observed photomagnetic effect is not due to a change in the magnetic exchange interaction but instead is due to the change in the absolute quantity of the magnetic moment. This explanation clearly suggests that the loss in d charge decreased in the case of the cis state and recovered in the case of the trans state. That is, the charge transfer from Au to S could be reversed with trans-to-cis photoisomerization.

These assumptions are also consistent with the reported cooperative effect of organic molecules in the electron transfer between a metal substrate and an organic layer. In such organic−inorganic interfaces, charge transfer acts to reduce the dipole−dipole interaction between molecules but may either decrease or increase the molecule-to-surface dipole moment.[10] The change $\Delta\Phi$ in the work function is related to the dipole moment density perpendicular to the surface through the following relationship:

$$\Delta\Phi = \frac{\mu N \cos\theta}{\varepsilon\varepsilon_0}$$

where N is the surface density of dipoles, μ is the effective dipole moment of the molecule, ε_0 is the permittivity of vacuum, ε is the dielectric constant of the layer, and θ is the tilt angle of the molecule with respect to the surface normal.[1a] In other words, the magnitude of the electron transfer to the organic layer becomes smaller for adsorbates with electronegative end groups, while it becomes larger for adsorbates with electropositive end groups. In fact, experimental evidence for such changes in the magnitude of the electron transfer from gold to the adsorbates has been reported previously.[10]

In the current system, the values of $\mu \cos\theta$ for AZ were calculated (using the corresponding MOPAC/PM3 geometries) as −0.52 D for the trans state and 1.77 D for the cis state, meaning that the sign of the work function change would be negative for the trans state and positive for the cis state. The tilt angles were taken to be 30° for both the trans and cis states. Hence, the magnitude of the electron transfer in the initial trans

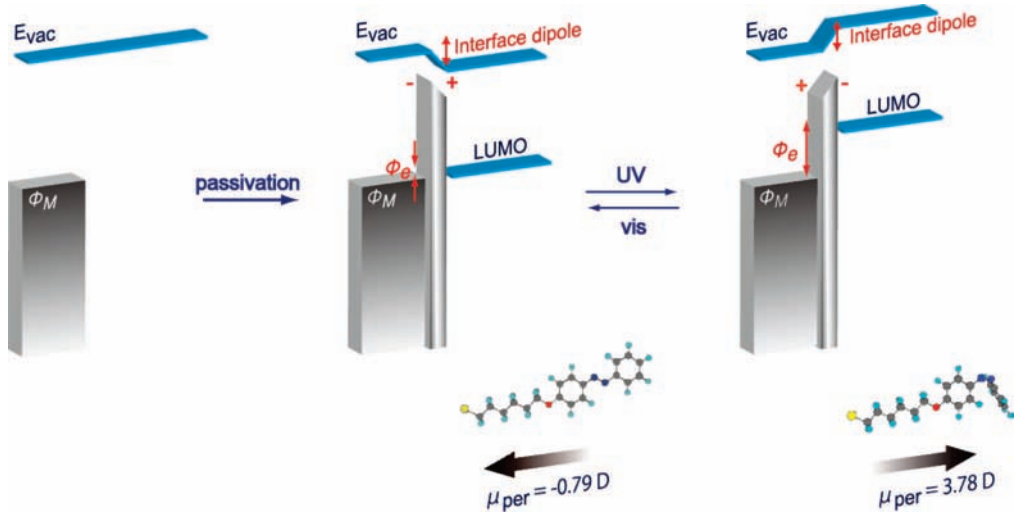

Figure 7. Schematic illustration of the changes in the work function due to photoisomerization of AZ: (left) schematic energy-level diagram for an untreated interface (without SAM formation); (middle) SAM formation by *trans*-AZ imposes an interface dipole that decreases the local vacuum energy level (E_{vac}); (right) photoisomerization to *cis*-AZ imposes an interface dipole that increases E_{vac}. In the diagrams, μ_{per} is the vertical component of the surface dipole, Φ_M is the metal work function, and Φ_e is the electron injection barrier.

state becomes smaller in the cis state under UV light illumination, and it recovers to its initial value under visible light illumination. To clarify this, we investigated the influence of photoillumination on the work function of the AZ-SAM by means of Kelvin probe analysis (Figure 6). During UV illumination, the initial value of the work function of the AZ-SAM (4.94 eV) increased to 5.53 eV. We then illuminated the AZ-SAM with visible light, and the work function decreased to near the initial state value. After this process, the UV-light-induced decrease and visible-light-induced increase in work function were repeated without attenuation. These observations provide clear evidence that the work function of AZ-SAM can be effectively controlled by photoisomerization by employing alternating photoillumination with UV and visible light. A schematic illustration of the change in work function due to photoisomerization of AZ is shown in Figure 7. As a consequence, the magnetization value at the Au−S interface can be controlled by employing alternating photoillumination with UV and visible light, and this is a result of the change in the loss of d charge resulting from the change in work function due to photoisomerization.

Conclusions

We have designed an azobenzene-containing self-assembled monolayer on a gold film. At the interface between the gold and the SAM, we observed the emergence of a large anisotropic magnetization as well as significant photoinduced changes in the magnetization value when alternating between UV and visible light illumination, showing that the value of the surface dipole moment changes due to photoisomerization. Furthermore, we also observed reversible changes in the work function of the gold film by illumination.

These photomagnetic effects can be attributed to photoinduced changes in the amount of charge transfer that result from photoisomerization of the azobenzene monolayer, which is accompanied by inversion of the surface dipoles.

As a result, we succeeded in controlling the magnetization by alternating the photoillumination between UV and visible light, and we have clarified the mechanism for the photomagnetic effects. A novel strategy such as this, which enables significant reversible phototuning of the magnetic order, has great potential for application in future magneto-optical devices.

Acknowledgment. This work was supported by a Grant-in-Aid for Scientific Research (A) and Scientific Research in Priority Areas "Photochromism (No. 471)" from the Ministry of Education, Culture, Sports, Science and Technology (MEXT) of the Japanese Government.

Supporting Information Available: XRD patterns, a schematic illustration of the AZ-SAM surface morphology, and an $M-H$ plot for the bare substrate. This material is available free of charge via the Internet at http://pubs.acs.org.

JA808231C